DOI: 10.1002/chem.200901847

Synthesis and Base Pairing Properties of 1′,5′-Anhydro-L-Hexitol Nucleic Acids (L-HNA)

Daniele D'Alonzo,[b] Arthur Van Aerschot,[a] Annalisa Guaragna,[b] Giovanni Palumbo,[b] Guy Schepers,[a] Stefania Capone,[b] Jef Rozenski,[a] and Piet Herdewijn*[a]

Abstract: Oligonucleotides composed of 1′,5′-anhydro-*arabino*-hexitol nucleosides belonging to the L series (L-HNA) were prepared and preliminarily studied as a novel potential base-pairing system. Synthesis of enantiopure L-hexitol nucleotide monomers equipped with a 2′-(N^6-benzoyladenin-9-yl) or a 2′-(thymin-1-yl) moiety was carried out by a de novo approach based on a domino reaction as key step. The L oligonucleotide analogues were evaluated in duplex formation with natural complements as well as with unnatural sugar-modified oligonucleotides. In many cases stable homo- and heterochiral associations were found. Besides T_m measurements, detection of heterochiral complexes was unambiguously confirmed by LC-MS studies. Interestingly, circular dichroism measurements of the most stable duplexes suggested that L-HNA form left-handed helices with both D and L oligonucleotides.

Keywords: DNA analogues · domino reactions · HNA · nucleic acids · oligonucleotides

Introduction

From the dawn of antisense research, the challenge of synthesising artificial nucleic acids has engaged chemists in the construction of a great number of oligonucleotide analogues that have more and more daring structural changes from the original model, but are capable of keeping the potential for selective cross communication.[1] One of the major efforts over the years has concerned the preparation of oligonucleotide architectures equipped with a sugar moiety deviating from the natural (deoxy)ribose backbone.[2] In some of these modifications, replacement of the five-membered furanose moiety with a six-membered ring, such as that present in pyranosyl nucleosides (homo-DNA,[3] Figure 1) has been designed to obtain highly preorganised structures towards duplex formation and resulted in potentially excellent candidates for cross pairing with natural complements.[4,5] One of the most prominent examples of this class of conformationally constrained oligonucleotide analogues is represented by the HNA system (1′,5′-anhydro-D-*arabino*-hexitol nucleic acids,[6] Figure 1), which has been found to hold great sequence-dependent RNA binding properties.[7] The great thermal stability exhibited by D-HNA-based duplexes has prompted research towards other base-pairing systems based on a six-membered sugar backbone, such as D-CNA,[8] D-ANA[9] and D-CeNA.[10]

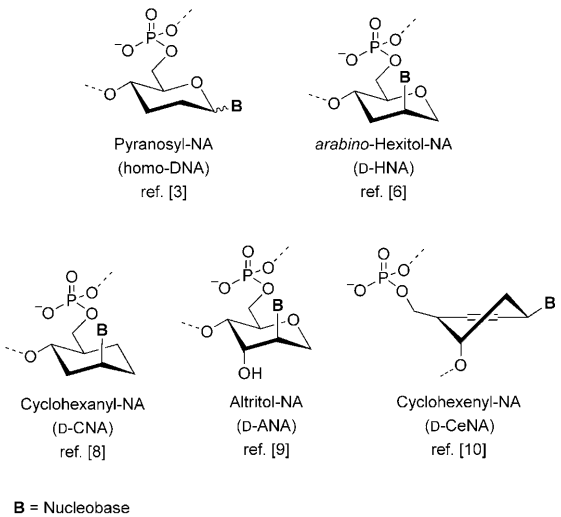

Figure 1. Sugar modified D series oligonucleotides.

[a] Prof. Dr. A. Van Aerschot, G. Schepers, Prof. Dr. J. Rozenski, Prof. Dr. P. Herdewijn
Rega Institute for Medical Research, Katholieke Universiteit Leuven
Minderbroederstraat 10, 3000 Leuven (Belgium)
Fax: (+32) 16-337340
E-mail: Piet.Herdewijn@rega.kuleuven.be

[b] Dr. D. D'Alonzo, Dr. A. Guaragna, Prof. G. Palumbo, Dr. S. Capone
Dipartimento di Chimica Organica e Biochimica
Università Federico II, Napoli, via Cinthia 4, 80126 Napoli (Italy)

Supporting information for this article is available on the WWW under http://dx.doi.org/10.1002/chem.200901847.

In this area, great opportunities were also provided by structures having the sugar moiety belonging to L-series (Figure 2). Some of them, such as L-LNA,[11] effectively displayed unprecedented hybridisation with both DNA and RNA complements. Studies involving modified L oligonucleotides (particularly L-CNA) were also carried out to examine the role of conformational diversity in the chiral selection of nucleic acid antipodes.[12] Recently, important findings arose from the use of L-DNA as oligonucleotide spiegelmers (from the German "Spiegel", for mirror) with many successful applications in the aptamer field[13] as well as in intracellular nucleic acid detection.[14] On the basis of these reports, our ongoing interest in sugar-modified oligonucleotides prompted us to examine the potential of L-hexitol nucleic acids (L-HNA, Figure 2) as a novel base-pairing system. In this paper, attention was primarily given to hybridisation properties of L-HNA with their natural complements; studies were also carried out to examine the hybridisation capacity of L-HNA with L-DNA[15] as well as with other D- and L-unnatural oligonucleotides.

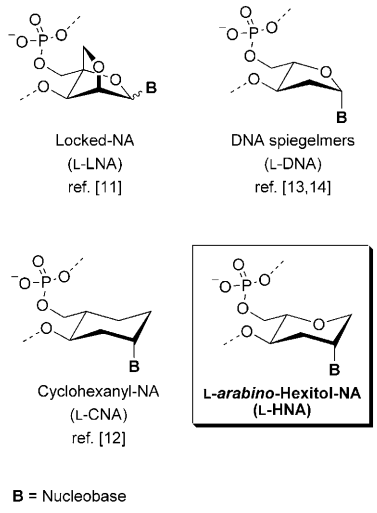

Figure 2. Sugar modified L series oligonucleotides.

Results and Discussion

Synthesis of L-hexitol-based nucleotide building blocks: The well-known poor commercial availability of almost all L-hexoses along with the small number of practical synthetic approaches[16] towards such compounds has long hampered the preparation of L-hexitol-based oligonucleotide analogues. Herein, synthesis of enantiopure L-hexitol nucleoside monomers **13** and **14** (Scheme 1) as building blocks for the preparation of L-HNA was carried out on the basis of a recently reported procedure[17] already devoted to L-hexose synthesis.[18] According to this strategy, construction of the 1,6-anhydrosugar backbone **2** was achieved by a domino reaction[19] by treating acetate **1** with DDQ (Scheme 1). Such a reaction involves five formal synthetic transformations in one step: MPM group removal, oxidation of the resulting primary alcohol, acetonide removal and acetalation by double intramolecular cyclisation (89%). Subsequently, dithioethylene bridge removal from **2**, followed by reductive cleavage of 1,6-anhydrosugar function of **3** afforded pseudoglucal **4** (55% yield over two steps). With the aim to create a *C*-2 electrophilic site for nucleobase insertion, **4** was first deacetylated, then the resulting allylic alcohol was stereoselectively epoxidized to provide oxirane **5** (89% overall yield). Finally, isopropylidene protection[20] of **5** afforded key intermediate **6** (80% yield).

With the protected epoxide **6** in our hand, nucleobase insertion into the required *C*-2′ axial position[21] was studied. Under mild basic conditions (DBU/DMF) both thymine and adenine L-altritol nucleosides **7** and **8** were obtained in good yields (89 and 74%, respectively; Scheme 1). Then, 3′-OH group removal in **7** and **8** under slightly modified Barton–McCombie conditions[17] promptly yielded the corresponding deoxynucleosides **10** (80% overall yield) and **12** (91% overall yield). Acetonide deprotection of the latter gave the pure 1′,5′-anhydro-2′-(thymin-1-yl)-2′,3′-dideoxy-L-*arabino*-hexitol (**13**) and 1′,5′-anhydro-2′-(adenin-9-yl)-2′,3′-dideoxy-L-*arabino*-hexitol (**14**) in quantitative yields (Scheme 1).

The analytical data of free nucleosides **13** and **14** obtained by ^{1}H and ^{13}C NMR spectroscopy, ESI-MS and CHNX analysis were identical to those of the corresponding D antipodes.[22] In addition, the absence of enantiomeric impurities[23] was confirmed by polarimetric measurements, and the optical rotations of nucleosides **13** and **14** were compared with those of the previously synthesised D antipodes (Scheme 1).

Incidentally, it must be noted that since some key enzymes involved in the development of viral infections are endowed with poor enantioselectivity,[24] nucleosides **13** and **14**, which have structures resembling L-nucleosides, were also considered with the aim to evaluate their antiviral potential.[25]

In order to examine the properties of L-hexitol nucleic acids, conversion of nucleosides **13** and **14** into fully protected phosphoramidite nucleotides was carried out (Scheme 2). The primary hydroxyl group of thymine nucleoside **13** was selectively protected (DMTCl/Py) to afford tritylated **15** (75%). Then, conversion into its phosphoramidite derivative **16** (DIPEA/2-cyanoethyl-*N*,*N*-diisopropyl chlorophosphoramidite) was easily achieved (74%). As far as adenine nucleoside **14** is concerned, transient protection[26] was used to selectively introduce the N^6-benzoyl group (99% yield), hence standard dimethoxytritylation of **17** and subsequent phosphoramidite installation in **18** afforded the fully protected nucleotide building block **19** (57% yield over two steps).

Oligonucleotide synthesis and hybridisation properties of L-HNAs: Assembly of **A***- and **T***-containing modified oligonucleotides (d($\mathbf{A}_L$*) and d($\mathbf{T}_L$*)) was accomplished by using the common phosphoramidite method on a solid support.[27] Fully modified sequences were assembled on a solid support containing a propane-1,3-diol linker. The 3′ tail generated did not interfere with physicochemical studies.[28] Several

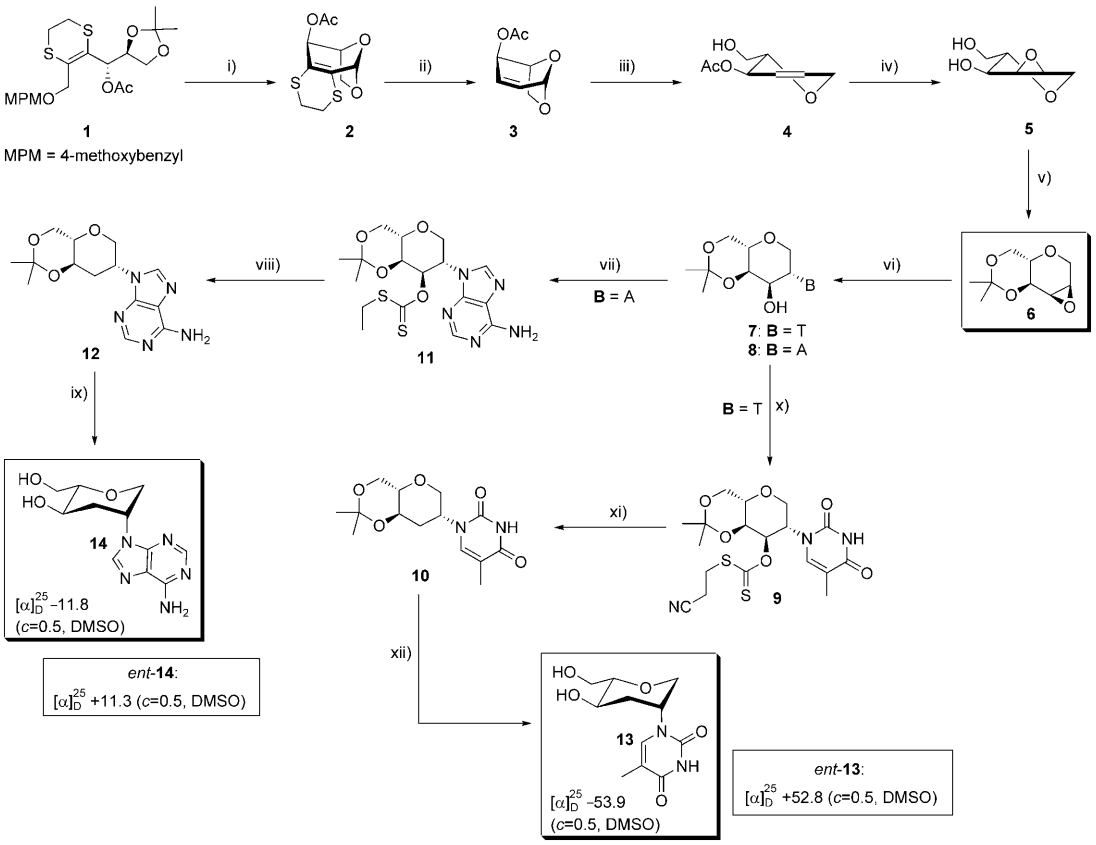

Scheme 1. Synthesis of L-*arabino*-hexitol nucleosides **13** and **14**. i) ref. [19], 89%; ii) Ra-Ni, acetone, room temperature, 70%; iii) TMSOTf, Et_3SiH, CH_2Cl_2, 0°C to room temperature, 78%; iv) a) MeONa, MeOH, room temperature, b) MCPBA, CH_2Cl_2, 0°C to room temperature, 89% overall yield; v) DMP, PPTS, acetone, room temperature, 80%; vi) T or A, DBU, DMF, 90°C, 6–8 h, 89 and 74%, respectively; vii) $NaOH_{aq}$, CS_2, $BrCH_2CH_3$, DMF, 0°C, 93%; viii) Bu_3SnH, AIBN, toluene, reflux, 15 min, 98%; ix) 80% $AcOH_{aq}$, 4 h, 60°C, quant.; x) $NaOH_{aq}$, CS_2, $BrCH_2CH_2CN$, DMSO, 0°C, 82%; xi) Bu_3SnH, AIBN, toluene, reflux, 15 min, 98%; xii) 80% $AcOH_{aq}$, 4 h, 60°C, quant.

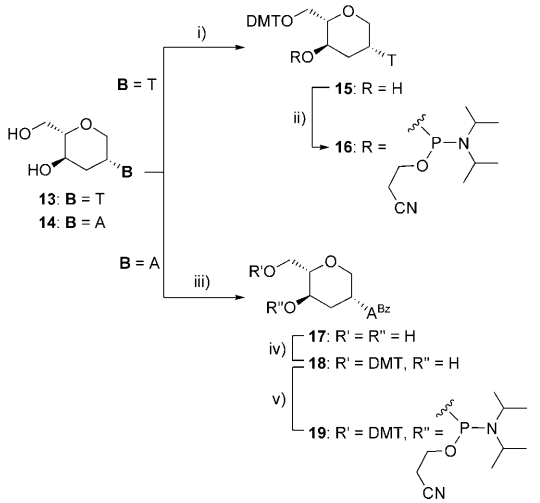

Scheme 2. Preparation of nucleotides **16** and **19** as building blocks for oligonucleotide synthesis. i) DMTCl, Py, 75%; ii) $(iPr)_2NP(Cl)(OCH_2CH_2CN)$, DIPEA, CH_2Cl_2, 74%; iii) TMSCl, BzCl, Py, 99%; iv) DMTCl, Py, 68%; v) $(iPr)_2NP(Cl)(OCH_2CH_2CN)$, DIPEA, CH_2Cl_2, 84%.

10–13-mer modified oligonucleotides were synthesised, including oligoadenylates, oligothymidylates and mixed adenine/thymine oligonucleotides. Deconvoluted electrospray ionisation mass spectrometric analysis showed all oligonucleotides to be of correct molecular weight (Table 1).

The pairing properties of L-HNA containing oligonucleotides were examined by hybridising oligomers with their complementary strands and determining the melting points (T_m) of the hybrids by temperature-dependent UV spectroscopy. To determine whether the presence of L-hexitol nucleosides into a short natural oligodeoxyribonucleotide sequence can perturb the structure of the corresponding DNA duplex, incorporation of a single thymine or adenine nucleoside **13** or **14** at the **X** position of the 5′-d(CACCG**X**TGCTACC)-3′ sequence was examined. The stability of the resulting duplexes was compared to those of the fully natural corresponding double stranded (ds) DNA. The strength of hybridisation was studied by thermal denaturation experiments, which were determined at 260 nm in NaCl (0.1 M) buffer with KH_2PO_4 (20 mM, pH 7.5) and EDTA (0.1 mM) at a concentration of 4 μM for each strand. Compared to the corresponding fully natural DNA strands, incorporation of a single nucleoside **13** or **14** into the matched sequence led to greatly reduced thermal stability of the resulting duplex (Table 2, entries 1 and 5). In particular, introduction of thymine nucleoside **13** (d(T_L*)) led to a T_m of 46.1°C (versus

Table 1. ESI-MS data of oligonucleotides containing L-hexitol nucleosides.

Entry	Sequence	MS calcd	MS found
1	5′-d(CAC CG**T**$_L$* TGC TAC C)	3882.7	3882.7
2	5′-d(CAC CG**A**$_L$* TGC TAC C)	3891.7	3891.7
3	5′-d(AGT ATT G**T**$_L$*C CTA)	3647.7	3647.7
4	5′-d(AGT ATT G**A**$_L$*C CTA)	3656.7	3656.7
5	6′-d(**T**$_L$*T$_L$*T$_L$* T$_L$*T$_L$*T$_L$* T$_L$*T$_L$*T$_L$*T$_L$* T$_L$*T$_L$*T$_L$*T$_L$* T$_L$*)	4210.9	4211.1
6	6′-d(**A**$_L$*A$_L$*A$_L$* A$_L$*A$_L$*A$_L$* A$_L$*A$_L$*A$_L$*A$_L$* A$_L$*A$_L$*A$_L$*A$_L$* A$_L$*)	4328.0	4328.3
7	6′-d(**A**$_L$*T$_L$*T$_L$* T$_L$*A$_L$*T$_L$* A$_L$*T$_L$*T$_L$* A$_L$*T$_L$*T$_L$* A$_L$*)	4255.9	4255.8
8	6′-d(**A**$_L$*T$_L$*A$_L$* A$_L$*A$_L$*T$_L$* T$_L$*T$_L$*A$_L$* T$_L$*)	3301.7	3301.9

d(**A**$_L$*): L-hexitol adenine nucleoside; d(**T**$_L$*): L-hexitol thymine nucleoside.

57.1 °C of natural dsDNA). Similarly, incorporation of the corresponding adenine nucleoside moiety **14** (d(**A**$_L$*)) led to a T_m of 45.4 °C (versus 57.0 °C of natural dsDNA). Single **T**$_L$*–T, **T**$_L$*–C and **T**$_L$*–G mismatches in this sequence were also introduced (Table 2, entries 2–4); this resulted in a decrease of ΔT_m values, ranging from 2.5 to 8.2 °C. Likewise, one **A**$_L$*–A, **A**$_L$*–C and **A**$_L$*–G mismatch led to a slight ΔT_m from −2.3 to −4.3 °C (entries 6–8).

Table 2. Hybridisation studies between the mixed DNA sequence 5′-d(CACCG**X**TGCTACC)-3′ and its natural complement 3′-d(GTGGC**Y**ACGATGG)-5′ after a single d(**T**$_L$*) or d(**A**$_L$*) incorporation, including mismatches.

Entry	**Y**	3′-d(CCA TCG T**X**G CCA C)-5′ 5′-d(GGT AGC A**Y**C GGT G)-3′ **X** = **T**$_L$*		**X** = T	
		T_m [°C]	ΔT_m [°C]	T_m [°C]	ΔT_m [°C]
1	A	46.1	–	57.1	–
2	T	39.9	−6.2	46.7	−10.4
3	C	37.9	−8.2	43.2	−13.9
4	G	43.6	−2.5	50.9	−6.2
Entry	**Y**	**X** = **A**$_L$*		**X** = A	
		T_m [°C]	ΔT_m [°C]	T_m [°C]	ΔT_m [°C]
5	T	45.4	–	57.0	-
6	A	43.0	−2.4	46.9	−10.1
7	C	41.1	−4.3	45.0	−12.0
8	G	43.1	−2.3	53.2	−3.8

In a second set of experiments, the pairing properties of fully modified L-HNA sequences were examined by hybridising the oligomers with both their natural complements and other unnatural oligonucleotides,[29] namely D- and L-cyclohexanyl-NA[8] (CNA), α- and β-D-hexopyranosyl-NA[30] (D-homo-DNA), D-HNA,[6] L-DNA[31] (Figures 1 and 2) and peptide-NA[32] (PNA). Synthesis of such unnatural sequences has already been reported elsewhere.[6,8,29–32] For most experiments, hybridisation was examined within the simplest recognition mode (oligoA vs. oligoT).[33] On the basis of our data and literature information, it is reasonable to assume the formation of double helices, even though the presence of triplexes or higher-order complexes cannot be fully excluded.

The stability of complexes formed by self complementary base pairing between d(**T**$_L$*)$_{13}$ and d(**A**$_L$*)$_{13}$ strands was studied first. Melting curves were compared to those of the corresponding D-hexitol oligonucleotides (D-HNA). Complexes between fully modified oligonucleotides and their natural complements were also considered.

L-HNA formed very stable homochiral self-complementary duplexes (ds-L-HNA) in agreement with those obtained with ds-D-HNA.[6] The complex between d(**T**$_L$*)$_{13}$ and d(**A**$_L$*)$_{13}$ gave the same melting profile (T_m 77 °C) as that of between d(**T**$_D$*)$_{13}$ and d(**A**$_D$*)$_{13}$ (T_m 78 °C). Both duplexes were significantly more stable than the corresponding natural complexes (dsDNA and DNA–RNA). The stereochemical relationship between D- and L-HNA was confirmed by circular dichroism (CD) experiments, in which the single CD spectra of the self complementary 6′-d(**A**$_L$*T$_L$*(**A**$_L$*)$_3$(**T**$_L$*)$_3$**A**$_L$*T$_L$*) sequence and of its D enantiomer exhibited a perfect mirror-image behaviour (Figure 3).[34]

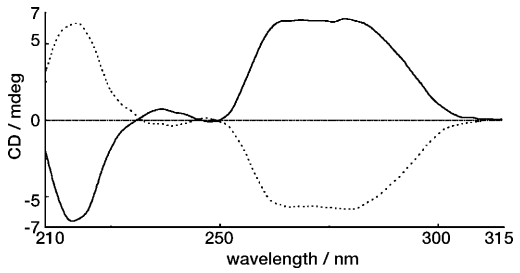

Figure 3. CD spectra of single strands related to 6′-d(**A**$_L$*T$_L$*(**A**$_L$*)$_3$-(**T**$_L$*)$_3$**A**$_L$*T$_L$*) (•••••) and its D enantiomer (——).

It is noteworthy that, besides A–T associations, T–T and A–A interactions were formed. In particular, a d(**T**$_L$*)$_{13}$–d-(**T**$_L$*)$_{13}$ association was found, and stability of the association was heavily dependent on salt buffer concentration (T_m values range from 33 to 51 °C with increasing NaCl concentration from 0.1 to 1 M; Table 3). This result fits with that found for the d(**T**$_D$*)$_{13}$–d(**T**$_D$*)$_{13}$ hybrid.[6] A somewhat weak d(**A**$_L$*)$_{13}$–d(**A**$_L$*)$_{13}$ association was also detected and its T_m linearly increased with salt concentration (Table 3). This is indicative for an intermolecular complex formation between d(**A**$_L$*)$_{13}$ strands, even though the broad melting curve does not suggest a single stable association.[35]

Much more unstable associations were found between L-HNA and the natural DNA and RNA. In particular, given the fact that d(**A**$_L$*)$_{13}$–dT$_{13}$ and d(**A**$_L$*)$_{13}$–dT$_2$rU$_{13}$dT$_2$ hybrids had the same melting profiles as well as similar T_m values (28–31 °C), it can be conjectured that such associations might be better related to a d(**A**$_L$*)$_{13}$–d(**A**$_L$*)$_{13}$ interaction. In the case of d(**T**$_L$*)$_{13}$–dA$_{13}$ and d(**T**$_L$*)$_{13}$–rA$_{13}$ associations, sigmoidal but broad melting curves did not suggest one clear transition.

Table 3. Thermal stability studies of duplexes containing L-HNA, D-HNA, D-DNA and D-RNA oligonucleotides. Melting points were determined at 260 nm (unless otherwise specified) in 0.1 M NaCl, 20 mM KH_2PO_4 (pH 7.5), 0.1 mM EDTA.

Entry	Oligomer (sequence)	Complement (T_m [°C])				Self hybridisation (T_m [°C])
		D-DNA	D-RNA	L-HNA	D-HNA	
1	D-DNA-d(T_{13})	34[a]	32	31[b]	21[a]	–
2	D-RNA-r(T_{13})	34[a]	ND	ND	ND	–
3	D-RNA-d($T_2rU_{13}dT_2$)	14	26[c]	28[b]	33[c]	–
4	L-HNA-d($\mathbf{T}_L$*)$_{13}$	29[d]	21[d]	77	37,[e] 53[f]	33,[e] 51[f]
5	D-HNA-d($\mathbf{T}_D$*)$_{13}$	58[a]	48[c]	40,[e] 55[f]	78[a]	33,[e] 46[a,f]
6	L-HNA-d($\mathbf{A}_L$*)$_{13}$	31[b]	28[b,h]	77	40,[e] 55[f]	31,[e] 41[f]
7	D-HNA-d($\mathbf{A}_D$*)$_{13}$	21[a]	33[c]	37,[e] 53[f]	78[a]	31,[e] 41[f]

ND: not determined; [a] taken from ref. [6]; [b] T_m related to d($\mathbf{A}_L$*)$_{13}$–d($\mathbf{A}_L$*)$_{13}$ interaction; [c] taken from ref. [33]; [d] very broad transition; [e] determined in 0.1 M NaCl; [f] determined in 1 M NaCl; [g] determined at 270 nm; [h] d($T_2rU_{13}dT_2$) used as complement.

The formation of hetero-oligomers between D- and L-HNA was then investigated. Equimolar amounts of d($\mathbf{T}_D$*)$_{13}$ and d($\mathbf{A}_L$*)$_{13}$ at 0.1 and 1 M NaCl were mixed and the sharp melting curves for the resulting mixture had higher T_m values (40 and 55 °C, respectively) than those related to ds-d($\mathbf{T}_D$*)$_{13}$ (33 and 46 °C) or ds-d($\mathbf{A}_L$*)$_{13}$ (31 and 41 °C). The same results were provided by the mirror-image mixture (Table 3). This might suggest the possibility of heterochiral complex formation. To ascertain this conjecture, we tested the mixed 6′-d($\mathbf{A}_L$*($\mathbf{T}_L$*)$_3\mathbf{A}_L$*$\mathbf{T}_L$*$\mathbf{A}_L$*($\mathbf{T}_L$*)$_2\mathbf{A}_L$*($\mathbf{T}_L$*)$_2\mathbf{A}_L$*) sequence[36] after hybridisation with complementary D-HNA sequences 6′-d($\mathbf{T}_D$*($\mathbf{A}_D$*)$_2\mathbf{T}_D$*($\mathbf{A}_D$*)$_2\mathbf{T}_D$*$\mathbf{A}_D$*$\mathbf{T}_D$*($\mathbf{A}_D$*)$_3\mathbf{T}_D$*) and 6′-d($\mathbf{T}_D$*($\mathbf{A}_D$*)$_3\mathbf{T}_D$*$\mathbf{A}_D$*$\mathbf{T}_D$*($\mathbf{A}_D$*)$_2\mathbf{T}_D$*($\mathbf{A}_D$*)$_2\mathbf{T}_D$*), which could also allow the determination of the orientation of complementary strands in the duplex. However, the melting curves of the mixtures had temperatures and shapes that were similar to those of the single strands. CD experiments of such D- and L-mixed A/T sequences were also carried out, but the spectrum of each D-HNA/L-HNA mixture appeared in fact as the sum of those of the separate strands, with Cotton effects that elide each other. Owing to these last results, regular Watson–Crick base pairing can be excluded, even though the possible formation of a complex between d($\mathbf{A}_L$*)$_{13}$ and d($\mathbf{T}_D$*)$_{13}$, as well as the mirror-image mixture, needed further examination with different experiments (see below for LC-MS studies).

L-HNA strands in either homopurine or homopyrimidine form were finally hybridised with the aforementioned unnatural complements, and showed, in some cases, from good to excellent hybridisation capacity (Table 4, Figure 4). In particular, high T_m values were found for the L-HNA–L-CNA duplexes (72 and 61 °C, Table 4, entries 1 and 2) in analogy with their D-HNA–D-CNA counterparts. On the other hand, no stable duplexes were detected after L-HNA–D-CNA hybridisation[37] (Table 4, entries 3 and 4). Interestingly, even though an obvious preferable aptitude for association with L oligomers occurred, a remarkable T_m value was found for the L-HNA-T_{13}–α-D-homo-DNA-A_{13} duplex (56 °C, Table 4, entry 5). The T_m values obtained after association between L-HNA-T_{13} and β-D-homo-DNA-A_{13} was even higher (78 °C, Table 4, entry 7). A very stable duplex was also detected after hybridisation between L-HNA-T_{13} and PNA-A_{10} (73 °C, Table 4, entry 9). Finally, it is worth mentioning that no stable association was found for the L-HNA–L-DNA duplex[38] (Table 4, entry 10). This result matches the aforementioned investigations[6] regarding the selectivity of D-HNA for D-RNA rather than D-DNA.

The high T_m values reported in Table 4 and Figure 4 for the interaction between modified oligonucleotides with the same

Table 4. T_m values of L-HNA with unnatural oligonucleotides. Data were compared to those related to associations with D-HNA.

Entry	Oligonucleotide (sequence)	Complement (T_m [°C])	
		L-HNA	D-HNA
1	L-CNA-d(A_L)$_{13}$	72	ND
2	L-CNA-d(T_L)$_{13}$	61	ND
3	D-CNA-d(A_D)$_{13}$	–	72[a]
4	D-CNA-d(T_D)$_{13}$	31.5[b,c]	62[a]
5	α-D-homo-DNA-d(A_D)$_{13}$	56	69[a]
6	α-D-homo-DNA-d(T_D)$_{13}$	30	64[a]
7	β-D-homo-DNA-d(A_D)$_{13}$	78	ND
8	β-D-homo-DNA-d(T_D)$_{13}$	35	62[a]
9	PNA-A_{10}	73	ND
10	L-DNA-d(T_L)$_{10}$	31[b,c]	ND

ND: not determined; [a] data from ref. [33]; [b] broad melting curve; [c] T_m is probably related to a d($\mathbf{A}_L$*)$_{13}$–d($\mathbf{A}_L$*)$_{13}$ interaction.

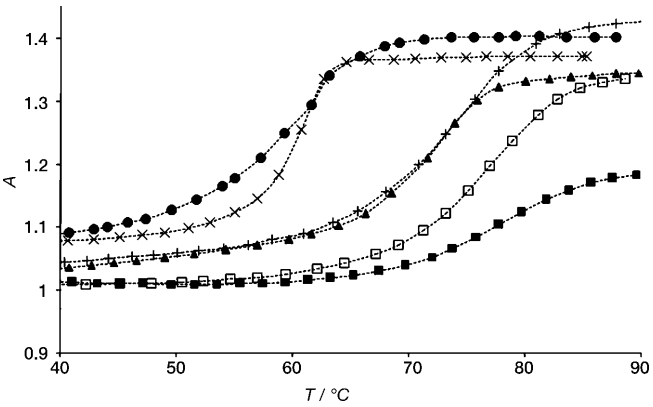

Figure 4. Melting curves for L-HNA based homo- and heterochiral oligomers: L-HNA-T_{13} mixed with α-D-homo-DNA-A_{13} (●); L-HNA-A_{13} mixed with L-CNA-T_{13} (×); L-HNA-T_{13} mixed with PNA-A_{10} (+); L-HNA-T_{13} mixed with L-CNA-A_{13} (▲); L-HNA-T_{13} mixed with L-HNA-A_{13} (□); L-HNA-T_{13} mixed with β-D-homo-DNA-A_{13} (■).

configuration can be explained by taking into account the high degree of preorganisation that six-membered oligonucleotides hold as a consequence of the relatively rigid chair structure of the sugar backbone. Also, the stable duplex formed between L-HNA and PNA confirms that PNA can adopt both left-handed and right-handed structures, depending on the configuration of its hybridisation partner.[12,32] On

the other hand, formation of double helices by oligonucleotides with opposite configuration was a much less predictable result, which has seldom been observed before[12] and needed to be more accurately confirmed. With this aim, CD experiments were carried out involving L-HNA–L-CNA, ds-L-HNA, L-HNA–β-D-homo-DNA and L-HNA–α-D-homo-DNA duplexes, which gave the most thermally stable complexes (Figures 5 and 6).

All these homo- and heterochiral mixtures gave CD spectra that were different from those of the corresponding single strands; this strongly suggests the formation of heterochiral complexes as indicated by the T_m studies. Moreover, it is noteworthy that spectra of all the examined mixtures had negative Cotton effects. In the case of ds-L-HNA and L-HNA–L-CNA duplexes (Figure 5) this result easily leads to the conclusion that these complexes form left-handed double helices.[39]

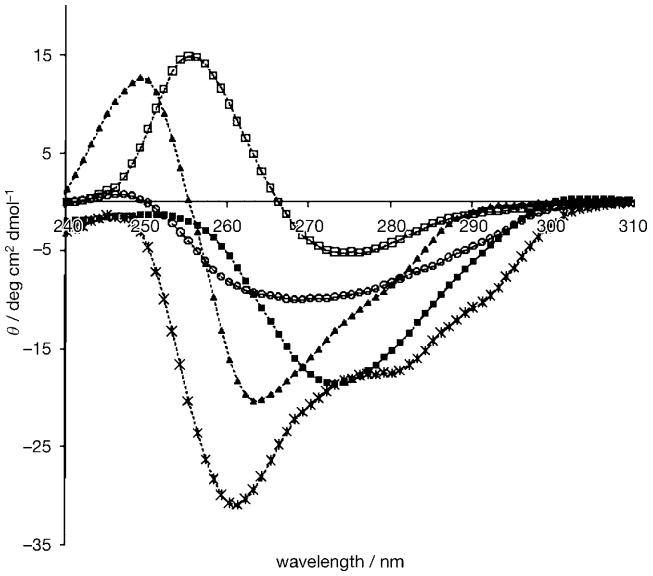

Figure 5. Normalised CD spectra of: L-HNA-A_{13} (□); L-HNA-T_{13} (■); L-HNA-A_{13}–L-HNA-T_{13} (○); L-CNA-A_{13} (▲); L-HNA-T_{13}–L-CNA-A_{13} (×). Measures were taken at 20 °C in 0.1 M NaCl, 20 mM KH_2PO_4 (pH 7.5), 0.1 mM EDTA.

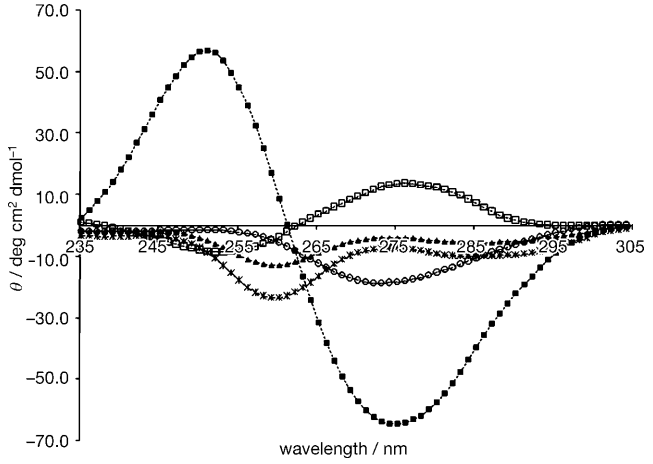

Figure 6. Normalised CD spectra of: L-HNA-T_{13} (○); α-D-homo-DNA-A_{13} (▲); β-D-homo-DNA-A_{13} (□); L-HNA-T_{13}–α-D-homo-DNA-A_{13} (×); L-HNA-T_{13}–β-D-homo-DNA-A_{13} (■). Measures were taken at 20 °C in 0.1 M NaCl, 20 mM KH_2PO_4 (pH 7.5), 0.1 mM EDTA.

On the other hand, in case of L-HNA–α-D-homo-DNA and of L-HNA–β-D-homo-DNA complexes (Figure 6) it can be only conjectured that, since L-CNA–β-D-homo-DNA duplex is in a left-handed form[12] and given the structural similarity between the CNA and HNA constructs, the negative Cotton effects should be related to duplexes existing in left-handed forms.

Detection of heterochiral complexes by LC-MS experiments: Even though T_m and CD studies already provided striking indications on the formation of heterochiral complexes, LC-MS experiments gave the final evidence that confirmed such interactions. Figure 7 shows the LC-MS behaviour of the complex formed between L-HNA-T_{13} and β-D-homo-DNA-A_{13}. LC profiles of the single oligothymidylate and oligoadenylate strands and of the corresponding mixture already showed different retention times; this clearly suggests an interaction. Interestingly, LC profile of β-D-homo-DNA-A_{13} displayed two peaks, MS analysis of which proved that they are related to the single strand ($[A]^{4-}$, m/z 1081.3; $[A]^{3-}$, m/z 1441.7) and to the duplex based on A–A interactions ($[A–A]^{5-}$, m/z 1730.4), respectively (Figure 7a). MS analysis of L-HNA-T_{13} also showed the faint signal of a T–T duplex[40] ($[T–T]^{5-}$, m/z 1683.7), in addition to the signals of the single strand ($[T]^{4-}$, m/z 1051.7; $[T]^{3-}$, m/z 1402.6; Figure 7b). Then, MS analysis of the L-HNA–β-D-homo-DNA complex revealed a major peak related to the A–T duplex ($[A–T]^{5-}$, m/z 1707.1), while the peak associated to A–A interaction had disappeared (Figure 7c).

LC-MS studies of the complex formed between L-HNA-T_{13} and α-D-homo-DNA-A_{13} demonstrated that the α-D-homo-DNA-A_{13} as single strand on its own also had a A–A interaction ($[A–A]^{5-}$, m/z 1730.4). Analysis of the L-HNA-T_{13}–α-D-homo-DNA-A_{13} complex mainly highlighted the peaks related to the single strands, even though three more weak signals associated with duplexes (ds-L-$(HNA-T)_{13}$, ds-α-D-$(homo-A)_{13}$ and L-$(HNA-T)_{13}$–α-D-$(homo-A)_{13}$) could be detected (see the Supporting Information).

Finally, in order to consider the interaction between L-HNA-A_{13} and D-HNA-T_{13}, which was suggested by T_m studies, LC-MS runs were carried out. LC-MS profile of L-HNA-A_{13} (Figure 8a) confirmed the existence of a duplex based on a A–A interaction ($[A–A]^{5-}$, m/z 1731.1) while the spectrum of D-HNA-T_{13} was identical to its mirror image (Figure 7b) and was not reported. Again, the LC profile of the mixture clearly demonstrated the occurrence of the interaction, owing to the different retention time compared to the single strands. The existence of the complex was then further confirmed by ESI-MS ($[A–T]^{5-}$, m/z 1707.6; Figure 8b).

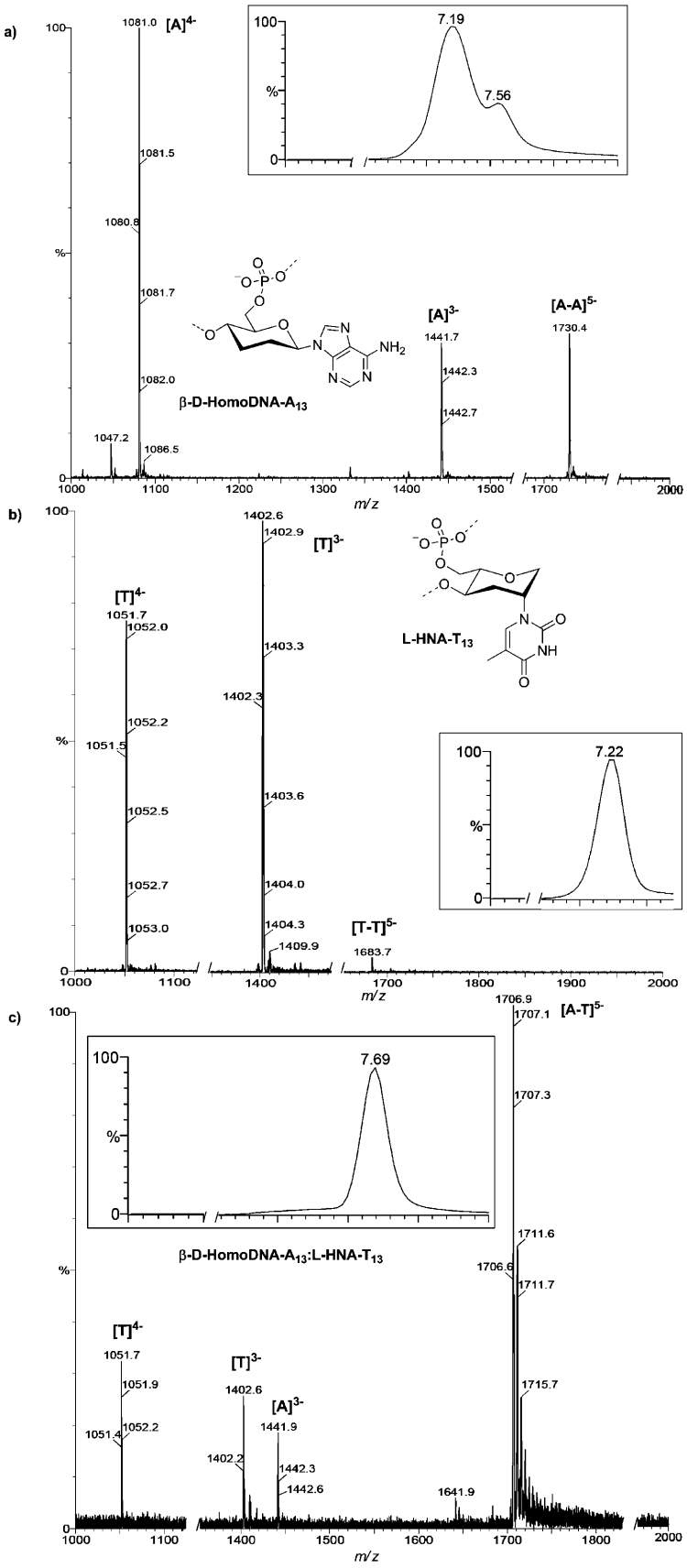

Figure 7. LC-MS profiles of β-D-homo-DNA-A_{13}, L-HNA-T_{13} and L-HNA-T_{13}–β-D-homo-DNA-A_{13}.

Conclusions

1′,5′-Anhydro-L-*arabino*-hexitol nucleic acids (L-HNA) with either thymine or adenine as the base moieties were prepared and studied. Synthesis of the corresponding L-hexitol nucleotide building blocks was carried out by a convenient and scalable de novo approach. As in the case of D-HNA, L-HNA oligonucleotides showed self association; the homochiral duplexes were significantly more stable than the corresponding natural associations. Moreover, even though the L-HNA system was found not to be able to hybridise with natural DNA and RNA (or at least not able to give a single stable interaction), strong associations were found after hybridisation with homochiral oligonucleotides with a six-membered sugar backbone. Remarkably, Pu–Py pairing was observed between L-HNA and hexose oligonucleotides with the D configuration. In addition, CD experiments seem to suggest that L-HNA always form left-handed helices, either with D or L oligonucleotides. Further in-depth examination of this topic is in progress; in particular, efforts are currently focusing on structure determination of L-HNA based duplexes, in order to provide new insight into the actual conformation of the hexitol backbone following double helix formation.

Experimental Section

Chemical synthesis of L-*arabino*-hexitol-based nucleotide building blocks: All moisture-sensitive reactions were performed under nitrogen atmosphere by using oven-dried glassware. Solvents were dried over standard drying agents and freshly distilled prior to use. Reactions were monitored by TLC (precoated silica gel

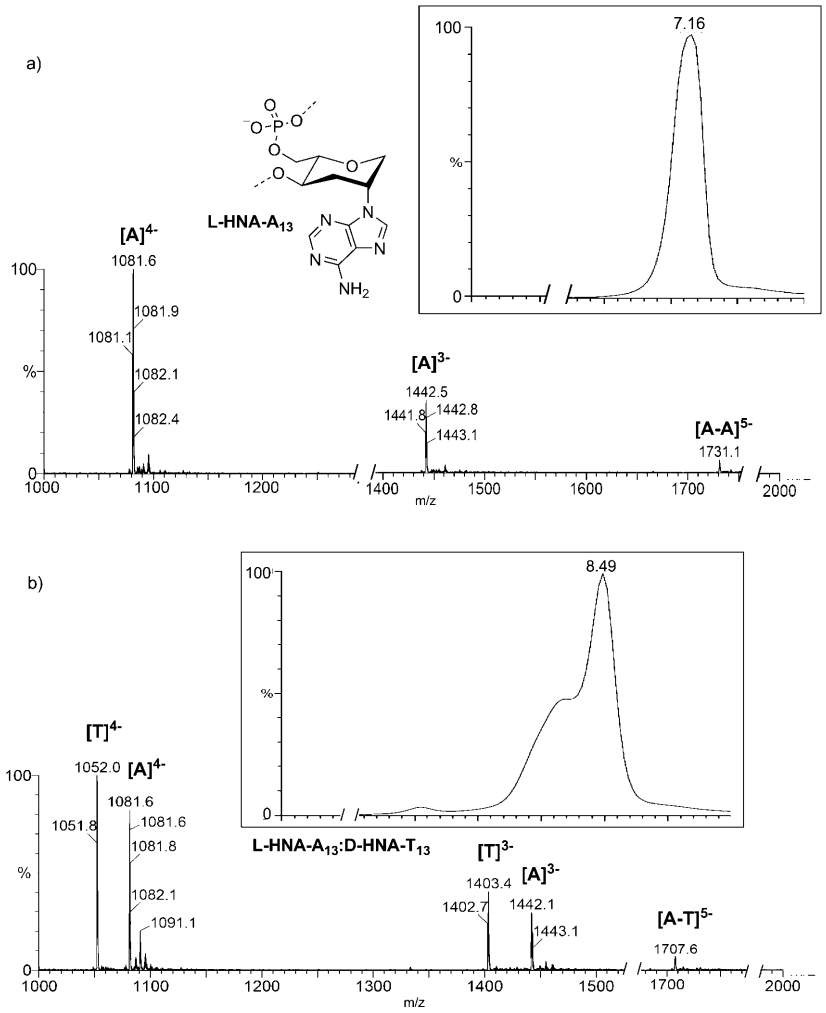

Figure 8. LC-MS profiles of L-HNA-A_{13} and D-HNA-T_{13}–L-HNA-A_{13}.

plate F254, Merck). Column chromatography: Merck Kieselgel 60 (70–230 mesh); flash chromatography: Merck Kieselgel 60 (230–400 mesh). Optical rotations were measured at (25±2)°C in the stated solvent. ^{1}H and ^{13}C NMR spectra were recorded on NMR spectrometers operating at 200, 300, 400 or 500 MHz and 50, 75, 100 or 125 MHz, respectively. Combustion analyses were performed by using CHNS analyzer. Exact mass measurements were performed by using a quadrupole time-of-flight mass spectrometer (Q-Tof-2, Micromass, Manchester, UK) equipped with a standard electrospray ionisation (ESI) interface.

4-*O*-Acetyl-1,6-anhydro-2,3-dideoxy-β-L-*erythro*-hex-2-enopyranose (3): A solution of **2** (4.0 g, 15.36 mmol; prepared according to ref. [19]) in acetone (200 mL) was added in one portion to a stirred suspension of Raney-Ni (W2; 40 g, wet; previously washed with H_2O) at 0°C and under nitrogen atmosphere. The suspension was stirred for 4 h, then the solid was filtered off and washed with acetone. The filtrate was evaporated under reduced pressure to afford a crude residue, which after chromatography over silica gel (CH_2Cl_2) gave pure **3** (1.96 g, 70%) as a colourless oil. $[\alpha]_D^{25}=-185.1$ ($c=2.0$ in $CHCl_3$); ^{1}H NMR (400 MHz, $CDCl_3$, 25°C): $\delta=2.12$ (s, 3H; CH_3CO), 3.54 (dd, $J_{6a,5}=2.1$, $J_{6a,6b}=8.0$ Hz, 1H; H-6a), 3.97 (dd, $J_{6b,5}=6.7$, $J_{6b,6a}=8.0$ Hz, 1H; H-6b), 4.71 (bdd, $J_{5,6a}=2.1$, $J_{5,6b}=6.7$ Hz, 1H; H-5), 4.80 (d, $J_{4,3}=4.4$ Hz, 1H; H-4), 5.60 (d, $J_{1,2}=3.5$ Hz, 1H; H-1), 5.81 (ddd, $J_{3,5}=1.7$, $J_{3,4}=4.4$, $J_{3,2}=9.6$ Hz, 1H; H-3), 6.20 ppm (dd, $J_{2,1}=3.5$, $J_{2,3}=9.6$ Hz, 1H; H-2); ^{13}C NMR (100 MHz, $CDCl_3$, 25°C): $\delta=21.1$ (CH_3), 63.2 (CH_2), 68.0 (CH), 74.7 (CH), 95.5 (CH), 122.5 (CH), 132.6 (CH), 170.6 ppm (CO); elemental analysis calcd (%) for $C_8H_{10}O_4$: C 56.47, H 5.92; found: C 56.28, H 5.94.

4-*O*-Acetyl-1,5-anhydro-2,3-dideoxy-L-*erythro*-hex-2-enitol (4): TfOTMS (0.34 mL, 1.89 mmol) was added dropwise to a stirring solution of 1,6-anhydrosugar derivative **3** (1.64 g, 9.64 mmol) and triethylsilane (2.11 mL, 13.20 mmol) in CH_2Cl_2 (60 mL) at 0°C. After 30 min, the reaction was quenched with solid $NaHCO_3$, heated to room temperature, diluted with CH_2Cl_2 (300 mL) and washed with brine (300 mL). The organic layer was dried (Na_2SO_4) and the solvent evaporated under reduced pressure. Chromatography of the crude residue over silica gel (CH_2Cl_2) gave the pure **4** (1.47 g; 78%) as a colourless oil. ^{1}H NMR (500 MHz, $CDCl_3$, 25°C): $\delta=2.12$ (s, 3H; CH_3CO), 3.49–3.54 (m, 1H; H-5), 3.58–3.63 (m, 1H; H-1a), 3.72–3.78 (m, 1H; H-1b), 4.18–4.25 (m, 2H; 2× H-6), 5.29 (brs, 1H, H-4), 5.76 (brd, $J_{3,2}=9.9$ Hz, 1H; H-3), 5.93 ppm (brd, $J_{2,3}=9.9$ Hz, 1H; H-2); ^{13}C NMR (100 MHz, $CDCl_3$, 25°C): $\delta=20.4$ (CH_3), 63.5 (CH_2), 64.5 (CH_2), 65.6 (CH), 78.7 (CH), 127.8 (CH), 128.9 (CH), 181.3 ppm (C); elemental analysis calcd (%) for $C_8H_{12}O_4$: C 55.81, H 7.02; found: C 55.68, H 7.19.

1,5:2,3-Dianhydro-L-*allo*-hexitol (5): Zemplén deacetylation was accomplished by treatment of **4** (1.20 g, 6.97 mmol) in MeOH (100 mL) with MeONa (0.75 g, 13.94 mmol) for 4 h at room temperature. Then the mixture was neutralised with acetic acid and the solvents were evaporated under reduced pressure. The crude residue was dissolved in $CHCl_3$ and filtered through a short pad of silica gel; the resulting filtrate was concentrated to dryness. The residue was dissolved in anhydrous CH_2Cl_2 (30 mL), then *m*CPBA (1.44 g, 8.36 mmol) was added at 0°C. The resulting reaction mixture was stirred at room temperature, overnight; then the insoluble materials were filtered off, washed and the filtrate was evaporated. Chromatography of the crude residue over silica gel (CH_2Cl_2/MeOH 9:1) gave pure **5** (0.98 g; 89% overall yield) as a colourless oil. $[\alpha]_D^{25}=-35.8$ ($c=1.0$, $CHCl_3$); ^{1}H NMR (500 MHz, CD_3OD, 25°C): $\delta=3.23$ (ddd, $J_{5,4}=2.0$, $J_{5,6a}=5.9$, $J_{5,6b}=8.8$ Hz, 1H; H-5), 3.40–3.43 (m, 1H; H-3), 3.51 (t, $J=4.2$ Hz, 1H; H-2), 3.55 (dd, $J_{6a,5}=5.9$, $J_{6a,6b}=11.7$ Hz, 1H; H-6a), 3.77–3.82 (m, 3H; H-4, H-6b, H-1a), 4.08 ppm (dd, $J_{1b,2}=4.2$, $J_{1b,1a}=13.2$ Hz, 1H; H-1b); ^{13}C NMR (125 MHz, CD_3OD, 25°C): $\delta=55.4$ (CH), 56.5 (CH), 63.1 (CH_2), 65.6 (CH_2), 66.8 (CH), 76.8 ppm (CH); elemental analysis calcd (%) for $C_6H_{10}O_4$: C 49.31, H 6.90; found: C 49.15, H 6.93.

4,6-*O*-Isopropylidene-1,5:2,3-dianhydro-L-*allo*-hexitol (6): 2,2-Dimethoxypropane (DMP, 1.05 mL, 10.09 mmol) and pyridinium *p*-toluenesulfonate (PPTS, 1.68 g, 6.69 mmol) were added to a solution of **5** (0.97 g, 6.69 mmol) in anhydrous acetone (50 mL) and the resulting reaction mixture was stirred for 12 h at room temperature. Then the solvent was evaporated, the crude residue dissolved in EtOAc and washed with saturated $NaHCO_3$ (2×300 mL) and brine (2×200 mL). The organic layer was dried (Na_2SO_4) and the solvent evaporated under reduced pressure. Chromatography of the crude residue over silica gel (CH_2Cl_2) gave pure **6** (1.01 g; 80%) as a colourless oil. $[\alpha]_D^{25}=+1.2$ ($c=0.7$, $CHCl_3$); ^{1}H NMR (400 MHz, C_6D_6, 25°C): $\delta=1.29$ (s, 3H; CH_3), 1.50 (s, 3H; CH_3), 2.68 (appt, $J_{2,1}=3.5$, $J_{2,3}=4.4$ Hz, 1H; H-2), 3.09 (brd, $J_{2,3}=4.4$ Hz, 1H; H-3), 3.55 (dd, $J_{1a,2}=3.5$, $J_{1a,1b}=13.4$ Hz, 1H; H-1a), 3.58 (t, $J_{6a,6b}=J_{6a,5}=$

10.3 Hz, 1H; H-6a), 3.65 (d, $J_{1b,1a}=13.4$ Hz, 1H; H-1b), 3.71–3.78 (m, 1H; H-5), 3.79–3.85 ppm (m, 2H; H-6b, H-4); ^{13}C NMR (125 MHz, C_6D_6, 25 °C): $\delta=18.8$ (CH_3), 29.3 (CH_3), 51.4 (CH), 52.6 (CH), 62.6 (CH_2), 64.2 (CH_2), 65.8 (CH), 71.2 (CH), 99.8 ppm (C); elemental analysis calcd (%) for $C_9H_{14}O_4$: C 58.05, H 7.58; found: C 58.24, H 7.54.

General procedure for nucleoside synthesis: Purine or pyrimidine nucleobase (6.21 mmol) and the epoxide **6** (2.68 mmol) were suspended in anhydrous DMF (7 mL) under nitrogen for 15 min at room temperature. Then 1,8-diazabicylo[5.4.0]undec-7-ene (DBU, 6.21 mmol) was added and the reaction mixture was heated at 90 °C for 6–8 h, after which the reaction was cooled to room temperature, quenched with NH_4Cl and concentrated. The residue was extracted with CH_2Cl_2 and washed with brine (3× 150 mL). The organic layer was dried (Na_2SO_4) and the solvent was evaporated under reduced pressure. Chromatography of the crude residue over silica gel (CH_2Cl_2/MeOH 98:2) gave the corresponding pure purine or pyrimidine nucleoside (74–89%). Data for 1′,5′-anhydro-4′,6′-*O*-isopropylidene-2′-deoxy-2′-(thymin-1-yl)-L-*altro*-hexitol (**7**): white powder, $[\alpha]_D^{25}=-36.7$ ($c=0.6$, $CHCl_3$); ^{1}H NMR (500 MHz, $CDCl_3$, 25 °C): $\delta=1.44$ (s, 3H; CH_3), 1.50 (s, 3H; CH_3), 1.97 (s, 3H; CH_3), 3.51 (d, $J_{OH,3'}=5.0$ Hz, 1H; OH), 3.67 (dd, $J_{4',3'}=2.7$, $J_{4',5'}=9.7$ Hz, 1H; H-4′), 3.76 (t, $J_{6'a,5'}=J_{6'a,6'b}=10.3$ Hz, 1H; H-6′a), 3.88–3.94 (m, 1H; H-5′), 3.98 (dd, $J_{6'b,5'}=5.3$, $J_{6'b,6'a}=10.3$ Hz, 1H; H-6′b), 4.03 (d, $J_{1'a,1'b}=13.7$ Hz, 1H; H-1′a), 4.07 (brs, 1H; H-3′), 4.34 (dd, $J_{1'b,2'}=3.4$, $J_{1'b,1'a}=13.7$ Hz, 1H; H-1′b), 4.49 (brt, $J_{2',1'b}=J_{2',3'}=3.4$ Hz, 1H; H-2′), 7.84 (s, 1H; H-6), 8.43 ppm (brs, 1H; NH); ^{13}C NMR (75 MHz, $CDCl_3$, 25 °C): $\delta=12.7$ (CH_3), 19.2 (CH_3), 28.9 (CH_3), 57.2 (CH), 62.3 (CH_2), 64.0 (CH_2), 66.0 (CH), 67.2 (CH), 69.2 (CH), 100.0 (C), 111.4 (C), 137.9 (CH), 151.3 (C), 164.3 ppm (C); elemental analysis calcd (%) for $C_{14}H_{20}N_2O_6$: C 53.84, H 6.45, N 8.97; found: C 53.85, H 6.49, N 8.99. Data for 1′,5′-anhydro-4′,6′-*O*-isopropylidene-2′-deoxy-2′-(adenin-9-yl)-L-*altro*-hexitol (**8**): white powder, $[\alpha]_D^{25}=-9.9$ ($c=1.3$, DMSO); ^{1}H NMR (300 MHz, [D$_6$]DMSO, 25 °C): $\delta=1.27$ (s, 3H; CH_3), 1.33 (s, 3H; CH_3), 3.52–3.60 (m, 1H; H-4′), 3.72–3.90 (m, 3H; H-5′, H-6′a, H-6′b), 4.00–4.10 (m, 1H; H-3′a), 4.18–4.29 (m, 2H; H-1′a, H-1′b), 4.52–4.56 (m, 1H; H-2′), 5.83 (d, $J=4.3$ Hz, 1H; 3′OH), 7.29 (brs, 2H; NH_2), 8.17 (s, 1H, H-8), 8.29 ppm (s, 1H; H-2); ^{13}C NMR (75 MHz, [D$_6$]DMSO, 25 °C): $\delta=19.5$ (CH_3), 29.4 (CH_3), 56.3 (CH), 62.0 (CH_2), 65.0 (CH_2), 65.8 (CH), 67.6 (CH), 69.4 (CH), 99.5 (C), 118.6 (C), 139.6 (CH), 150.0 (C), 153.0 (CH), 156.5 ppm (C); elemental analysis calcd (%) for $C_{14}H_{19}N_5O_4$: C 52.33, H 5.96, N 21.79; found: C 52.15, H 5.98, N 21.85.

1′,5′-Anhydro-4′,6′-*O*-isopropylidene-2′-(thymin-1-yl)-2′,3′-dideoxy-L-*arabino*-hexitol (10): Aqueous NaOH (5N; 2.55 mL), CS_2 (2.55 mL) and then β-bromopropionitrile (6.1 mL) were added at 0 °C to a stirring solution of compound **7** (0.75 g, 2.41 mmol) in DMSO (15 mL). After being stirred for 30 min, the solvent was evaporated and the crude residue was extracted with CH_2Cl_2 and washed with NH_4Cl solution. The organic layer was dried (Na_2SO_4) and the solvent removed under reduced pressure to give crude **9**. To a refluxing solution of **9** dissolved in anhydrous toluene (25 mL), kept under nitrogen flow, a solution of nBu$_3$SnH (0.48 mL, 1.78 mmol) and AIBN (0.01 g, 0.06 mol) in anhydrous toluene (20 mL) was added dropwise over 1 h. After the addition, the brown solution was stirred for an additional 30 min under reflux. The reaction mixture was then concentrated under reduced pressure and the resulting residue was purified by column chromatography on silica gel (CH_2Cl_2/MeOH 95:5) to give the pure **10** (0.51 g, 1.70 mmol, 80% overall yield) as a white powder: $[\alpha]_D^{25}=-51.5$ ($c=0.3$, $CHCl_3$); ^{1}H NMR (300 MHz, $CDCl_3$, 25 °C): $\delta=1.70$ (s, 3H; CH_3), 1.75 (s, 3H; CH_3), 1.92 (ddd, $J_{3'a,2'a}=4.7$, $J_{3'a,4'}=12.6$, $J_{3'a,3'b}=13.3$ Hz, 1H; H-3′a), 1.99 (s, 3H; CH_3), 2.28 (brd, $J_{3'b,3'a}=13.3$ Hz, 1H; H-3′b), 3.35 (ddd, $J_{5',6'b}=5.3$, $J_{5',4'}=9.7$, $J_{5',6'a}=10.1$ Hz, 1H; H-5′), 3.68–3.82 (m, 2H; H-4′, H-6′a), 3.92–4.02 (m, 2H; H1′a, H6′b), 4.20 (brd, 1H, $J_{1'b,1'a}=14.0$ Hz), 4.62 (brs, 1H; H-2′), 7.84 (s, 1H; H-6), 8.65 ppm (s, 1H, NH); ^{13}C NMR (75 MHz, $CDCl_3$, 25 °C): $\delta=12.8$ (CH_3), 19.1 (CH_3), 29.1 (CH_3), 33.4 (CH_2), 51.5 (CH), 62.3 (CH_2), 66.0 (CH_2), 68.9 (CH), 75.5 (CH), 99.8 (C), 110.6 (C), 138.0 (CH), 150.7 (C), 163.4 ppm (C); elemental analysis calcd (%) for $C_{14}H_{20}N_2O_5$: C 56.75, H 6.80, N 9.45; found: C 56.91, H 6.78, N 9.41.

1′,5′-Anhydro-4′,6′-*O*-isopropylidene-2′-(adenin-9-yl)-2′,3′-dideoxy-L-*arabino*-hexitol (12): Aqueous NaOH (5N; 2.79 mL), CS_2 (2.79 mL) and then bromoethane (0.81 mL) were added at 0 °C to a stirring solution of compound **8** (0.81 g, 2.52 mmol) in DMF (33 mL). After being stirred for 30 min, the solvent was evaporated under reduced pressure; the crude residue was extracted with CH_2Cl_2 and washed with NH_4Cl solution. The organic layer was dried (Na_2SO_4) and the solvent evaporated to give crude **11**. To a refluxing solution of **11** dissolved in anhydrous toluene (60 mL) and kept under a nitrogen flow, a solution of nBu$_3$SnH (1.02 mL, 3.78 mmol) and AIBN (0.02 g, 0.1 mmol) in anhydrous toluene (60 mL) was added dropwise over 1 h. After the addition, the brown solution was stirred for an additional 30 min under reflux. The reaction mixture was then concentrated under reduced pressure and the resulting residue was purified by column chromatography on silica gel (CH_2Cl_2/MeOH 95:5) to give pure **12** (0.72 g, 85% over two steps) as a white brilliant powder: $[\alpha]_D^{25}=-19.7$ ($c=0.4$, $CHCl_3$); ^{1}H NMR (300 MHz, $CDCl_3$, 25 °C): $\delta=1.42$ (s, 3H; CH_3), 1.48 (s, 3H; CH_3), 2.05 (ddd, $J_{3'a,2'}=4.3$, $J_{3'a,4'}=11.8$, $J_{3'a,3'b}=13.5$ Hz, 1H; H3′a), 2.40–2.52 (m, 1H; H3′b), 3.44 (ddd, $J_{5',6'b}=5.2$, $J_{5',4'}=9.6$, $J_{5',6'a}=10.4$ Hz, 1H; H-5′), 3.73 (ddd, $J_{4',3'b}=4.5$, $J_{4',5'}=9.6$, $J_{4',3'a}=11.8$ Hz, 1H; H-4′), 3.82 (t, $J_{6'a,5'}=J_{6'a,6'b}=10.4$ Hz, 1H; H-6′a), 3.99 (dd, $J_{6'b,5'}=5.2$, $J_{6'b,6'a}=10.4$ Hz, 1H; H-6′b), 4.12 (dd, $J_{1'a,2'}=2.9$, $J_{1'a,1'b}=13.0$ Hz, 1H; H-1′a), 4.42 (brd, $J_{1'b,1'a}=13.0$ Hz, 1H; H-1′b), 4.94–5.00 (m, 1H; H-2′), 5.60 (brs, 2H; NH_2), 8.34 (s, 1H; H-8), 8.39 ppm (s, 1H; H-2); ^{13}C NMR (75 MHz, $CDCl_3$, 25 °C): $\delta=19.1$ (CH_3), 29.1 (CH_3), 33.7 (CH_2), 50.7 (CH), 62.4 (CH_2), 66.3 (CH_2), 69.8 (CH), 75.8 (CH), 99.8 (C), 117.7 (C), 139.7 (CH), 150.0 (C), 153.1 (CH), 155.4 ppm (C); elemental analysis calcd (%) for $C_{14}H_{19}N_5O_3$: C 55.07, H 6.27, N 22.94; found: C 55.24, H 6.25, N 22.85.

1′,5′-Anhydro-2′-(thymin-1-yl)-2′,3′-dideoxy-L-*arabino*-hexitol (13): A solution of nucleoside **10** (0.5 g, 1.69 mmol) in 80% AcOH (14 mL) was heated at 65 °C for 2 h. The reaction mixture was then concentrated to dryness under reduced pressure and the residue was coevaporated with a mixture of toluene and EtOH (1:1 *v*/*v*, 5×50 mL). The residue was purified by column chromatography (CH_2Cl_2/MeOH 9:1) to yield thymine nucleoside **13** (0.43 g, 99%) as white crystals: $[\alpha]_D^{25}=-53.9$ ($c=0.5$, DMSO); ^{1}H and ^{13}C NMR spectroscopy data coincide with those reported in refs. [6,19]; elemental analysis calcd for $C_{11}H_{16}N_2O_5$: C 51.56, H 6.29, N 10.93; found: C 51.68, H 6.31, N 10.89.

1′,5′-Anhydro-2′-(adenin-9-yl)-2′,3′-dideoxy-L-*arabino*-hexitol (14): A solution of nucleoside **12** (0.49 g, 1.62 mmol) in 80% AcOH (10 mL) was heated at 65 °C for 2 h while being stirred. Then the reaction mixture was concentrated to dryness and the residue was purified by column chromatography (CH_2Cl_2/MeOH 9:1) to yield adenine nucleoside **14** (0.42 g, 99%) as white crystals: $[\alpha]_D^{25}=-11.8$ ($c=0.5$, DMSO); ^{1}H and ^{13}C NMR spectroscopy data coincide with those reported in refs. [6,19]; elemental analysis calcd for $C_{11}H_{15}N_5O_3$: C 49.81, H 5.70, N 26.40; found: C 49.94, H 5.72, N 26.31.

1′,5′-Anhydro-2′-(N^6-benzoyladenin-9-yl)-2′,3′-dideoxy-L-*arabino*-hexitol (17): TMSCl (1.8 mL, 15.1 mmol) was added to a stirring solution of nucleoside **14** (0.4 g, 1.51 mmol) in anhydrous pyridine (30 mL) and under nitrogen atmosphere. After 30 min, BzCl (0.42 mL, 3.75 mmol) was added at 0 °C. The resulting reaction mixture was warmed to room temperature and further stirred for 16 h. Then H_2O (3 mL) was added at 0 °C and then NH_4OH (3 mL) after 10 min. The reaction mixture was stirred at the same temperature for 1 h; afterwards the solvent was removed under reduced pressure. Chromatography of the crude residue (CH_2Cl_2/MeOH 9:1) afforded the pure benzoylated nucleoside **17** (0.56 g, 99%) as a white powder. ^{1}H NMR (300 MHz, [D$_6$]DMSO, 25 °C): $\delta=1.96$–2.15 (m, 1H; H-3′a), 2.49–2.62 (m, 1H; H-3′b), 3.59–3.73 (m, 1H; H-5′), 3.80 (dd, $J_{6'a,5'}=4.9$, $J_{6'a,6'b}=12.0$ Hz, 1H; H-6′a), 3.91 (dd, $J_{6'b,5'}=2.2$, $J_{6'b,6'a}=12.0$ Hz, 1H; H-6′b), 4.08 (dd, $J_{1'a,2'}=2.3$, $J_{1'a,1'b}=12.9$ Hz, 1H, H-1′a), 4.42 (d, $J_{1'b,1'a}=12.9$ Hz, 1H; H-1′b), 4.61–4.74 (m, 1H; H-4′), 5.05 (brs, 1H, H-2′), 7.57 (t, $J_{ortho}=7.5$ Hz, 2H; H-arom), 7.66 (t, $J_{ortho}=7.5$ Hz, 1H; H-arom), 8.10 (d, $J_{ortho}=7.5$ Hz, 2H; H-arom), 8.72 (s, 1H; H-8), 8.78 ppm (s, 1H; H-2); ^{13}C NMR (75 MHz, [D$_6$]DMSO, 25 °C): $\delta=35.8$ (CH_2), 51.6 (CH), 61.0 (CH_2), 61.2 (CH_2), 68.3 (CH), 83.2 (CH), 123.0 (C), 128.0 (CH), 128.4 (CH), 132.6 (CH), 133.6 (C), 143.6 (CH), 149.6 (C), 151.6 (CH), 152.3 (C), 166.8 ppm (C); exact mass calcd for $C_{18}H_{19}N_5O_4$ [M+H]$^+$: 370.1509; found: 370.1511.

General procedure for nucleoside dimethoxytritylation: Dimethoxytrityl chloride (2.34 mmol) was added at room temperature to a solution of the nucleoside (1.95 mmol) in anhydrous pyridine (10 mL) and under nitrogen atmosphere. After being stirred at room temperature for 3 h, saturated $NaHCO_3$ solution (1 mL) was added, the reaction solvent was evaporated and the resulting residue was diluted with CH_2Cl_2 (50 mL) and washed with brine (3×50 mL). The organic layer was dried (Na_2SO_4), evaporated under reduced pressure and the crude residue was purified by flash chromatography (CH_2Cl_2/MeOH 98:2) to afford the corresponding dimethoxytritylated nucleoside (70–75%) as a white foam. ^1H and ^{13}C NMR data for 1′,5′-anhydro-6′-*O*-dimethoxytrityl-2′-(thymin-1-yl)-2′,3′-dideoxy-L-*arabino*-hexitol (**15**) and 1′,5′-anhydro-6′-*O*-dimethoxytrityl-2′-(N^6-benzoyladenin-9-yl)-2′,3′-dideoxy-L-*arabino*-hexitol (**18**) coincide with those reported in ref. [6]. Exact mass calcd for thymine nucleoside **15**: $C_{32}H_{34}N_2O_7$ $[M+H]^+$: 559.2444, found 559.2433. Exact mass calcd for adenine nucleoside **18**: $C_{39}H_{37}N_5O_6$ $[M+H]^+$: 672.2822, found 672.2788.

General procedure for nucleoside phosphitylation: Freshly dried diisopropylethylamine (3.3 mmol) and 2-cyanoethyl-*N*,*N*-diisopropyl chlorophosphoramidite (1.6 mmol) were added to a solution of the dimethoxytritylated nucleoside (1 mmol) in anhydrous CH_2Cl_2 (6 mL) at 0°C and under argon atmosphere. The reaction mixture was stirred at 0°C for 90 min after the reaction was completed, as indicated by TLC. Saturated $NaHCO_3$ solution (2 mL) was added, the solution was stirred for another 10 min and partitioned between CH_2Cl_2 (50 mL) and aqueous $NaHCO_3$ (30 mL). The organic layer was washed with brine (3×30 mL) and the aqueous phases were extracted with CH_2Cl_2 (30 mL). After solvent evaporation, the resulting oil was purified by flash chromatography (hexane/acetone/TEA 62:36:2). The yellow solid was then dissolved in CH_2Cl_2 (3 mL) and precipitated twice in cold hexane (160 mL, −60°C) to afford the desired corresponding phosphoramidite nucleoside (74% yield for compound **16**, 84% yield for compound **19**) as a white powder. Each product was dried under vacuum and stored, overnight, under nitrogen at −20°C. Data for compound **16**: exact mass calcd for $C_{41}H_{51}N_4O_8P$ $[M+H]^+$: 759.3522, found 759.3510; ^{31}P NMR: $\delta=148.41$, 148.87 ppm. Data for compound **19**: exact mass calcd for $C_{48}H_{54}N_7O_7P$: $[M+H]^+$: 872.3900, found 872.3887; ^{31}P NMR: $\delta=148.40$, 148.67 ppm.

Oligonucleotide synthesis: Oligonucleotide assembly was performed with an Expedite DNA synthesizer (Applied Biosystems) by using the phosphoramidite approach. The oligomers were deprotected and cleaved from the solid support by treatment with methylamine (40% in water) and concentrated aqueous ammonia (1:1, 30°C). After gel filtration on a NAP-10 column (Sephadex G25-DNA grade; Pharmacia) with water as eluent, the crude mixture was analysed by using a Mono-Q HR 5/5 anion exchange column, after which purification was achieved by using a Mono-Q HR 10/10 column (Pharmacia) with the following gradient system: A = 10 mM NaOH, pH 12.0, 0.1 M NaCl; B = 10 mM NaOH, pH 12.0, 0.9 M NaCl. The low-pressure liquid chromatography system consisted of a Merck–Hitachi L-6200 A intelligent pump, a Mono-Q HR 10/10 column (Pharmacia), a Uvicord SII 2138 UV detector (Pharmacia-LKB) and a recorder. The product-containing fraction was desalted on a NAP-10 column and lyophilised. Oligonucleotides were purified by RP-HPLC on a C-18 column prior to mass spectrometric analysis. A linear gradient of A: ammonium bicarbonate (25 mM in H_2O, pH 7.0), and B: acetonitrile (80% in H_2O) was applied.

Characterisation of oligonucleotides by mass spectrometry: The purity of the oligonucleotides was checked by HPLC/MS on a capillary chromatograph (CapLC, Waters, Milford, MA, USA). Columns of 150 mm × 0.3 mm length (LC Packings, San Francisco, CA, USA) were used. Oligonucleotides were eluted with a triethylammonium/1,1,1,3,3,3-hexafluoro-2-propanol/acetonitrile solvent system; flow rate was 5 μL min^{-1}. Electrospray spectra were acquired by using an orthogonal acceleration/time-of-flight mass spectrometer (Q-Tof-2, Micromass, Manchester, UK) in negative ion mode; scan time used was 2 s. The combined spectra from a chromatographic peak were deconvoluted by using the MaxEnt algorithm of the software (Masslynx 3.4, Micromass, Manchester, UK). Theoretical oligonucleotide masses were calculated by using the monoisotopic element masses.

UV melting experiments: Oligomers were dissolved in a buffer solution containing NaCl (0.1 M), potassium phosphate (0.02 M, pH 7.5) and EDTA (0.1 mM). The concentration was determined by measuring the absorbance in MilliQ water at 260 nm at 80°C, and by assuming that hexitol nucleosides have the same extinction coefficients per base moiety in the denatured state as the natural nucleosides (A*, $\varepsilon=15\,000$; T*, $\varepsilon=8500$). The concentration for each strand was 4 μM in all experiments. Melting curves were determined with a Varian Cary 300 BIO spectrophotometer. Cuvettes were maintained at constant temperature by water circulation through the cuvette holder. The temperature of the solution was measured with a thermistor that was directly immersed in the cuvette. Temperature control and data acquisition were carried out automatically with an IBM-compatible computer by using Cary WinUV thermal application software. A quick heating and cooling cycle was carried out to allow proper annealing of both strands. The samples were then heated from 10 to 80°C at a rate of 0.2°C min^{-1}, and were cooled again at the same speed. Melting temperatures were determined by plotting the first derivative of the absorbance as a function of temperature; data plotted were the average of two runs. Up and down curves in general showed identical T_m values.

Circular dichroism measurements: CD spectra were measured at 20°C with a Jasco J-715 spectropolarimeter equipped with a Peltier-type temperature control system (model PTC-348WI) in thermostatically controlled 0.1 cm cuvettes. The molar ellipticity $[\theta]$ (deg cm^2 dmol^{-1}) was calculated from the equation: $[\theta]=[\theta]_{obs}\times(mrw)/10\times lc$, where $[\theta]_{obs}$ is the ellipticity (deg), mrw is the sample molecular weight (g mol^{-1}), c is the sample concentration (g mL^{-1}), l is the optical path length of the cell (cm). The cells had a 0.1 cm path length and sample concentration was about 0.16 mg mL^{-1}. The oligomers were dissolved and analysed in buffer containing NaCl (0.1 M), potassium phosphate (0.2 M, pH 7.5) and EDTA (0.1 mM).

LC-MS experiments: Oligonucleotides were dissolved at a concentration of 100 μM in H_2O containing HCO_2NH_4 (1 M). Samples (100 nL) were injected on a reverse phase column (C18 PepMap 0.5 × 15 mm, Dionex) and eluted with a *N*,*N*-dimethylaminobutane/1,1,3,3,3-hexafluoro-2-propanol and acetonitrile system. As reported above, electrospray spectra were acquired by using an orthogonal acceleration/time-of-flight mass spectrometer (Q-Tof-2, Micromass, Manchester, UK) in negative ion mode.

Acknowledgements

The authors are grateful to K. U. Leuven (OT) for financial support. D.D. is indebted to Paola Carullo and Luigi Martino for helpful discussions on CD experiments. CD measurements as well as most ^1H and ^{13}C NMR spectroscopy experiments were performed at Centro Interdipartimentale di Metodologie Chimico-Fisiche (CIMCF), Università di Napoli Federico II. The Varian Inova 500 MHz instrument is the property of Consorzio Interuniversitario Nazionale La Chimica per l'Ambiente (INCA) and was used in the frame of a project by INCA and M.I.U.R. (L. 488/92, Cluster 11 A).

[1] a) E. Uhlmann, A. Peyman, *Chem. Rev.* **1990**, *90*, 543–584; b) A. De Mesmaeker, R. Haener, P. Martin, H. E. Moser, *Acc. Chem. Res.* **1995**, *28*, 366–374; c) E. T. Kool, *Chem. Rev.* **1997**, *97*, 1473–1488; d) T. Aboul-Fadl, *Curr. Med. Chem.* **2005**, *12*, 2193–2214.
[2] C. J. Leumann, *Bioorg. Med. Chem.* **2002**, *10*, 841–854.
[3] a) M. Böhringer, H. J. Roth, J. Hunziker, M. Gobel, R. Krishnan, A. Giger, B. Schweizer, J. Schreiber, C. Leumann, A. Eschenmoser, *Helv. Chim. Acta* **1992**, *75*, 1416–1477; b) M. Froeyen, E. Lescrinier, L. Kerremans, H. Rosemeyer, F. Seela, B. Verbeure, I. Lagoja, J. Rozenski, A. Van Aerschot, R. Busson, P. Herdewijn, *Chem. Eur. J.* **2001**, *7*, 5183–5194.
[4] For a general perspective on the conformational diversity produced by oligonucleotides with a six-membered sugar backbone, see: E.

Lescrinier, M. Froeyen, P. Herdewijn, *Nucleic Acids Res.* **2003**, *31*, 2975–2989.

[5] The role of pyranose oligonucleotides has also been widely examined in discussions dealing with the chemical etiology of nucleic acids, see: a) A. Eschenmoser, *Science* **1999**, *284*, 2118–2124; b) A. Eschenmoser, *Chimia* **2005**, *59*, 836–850.

[6] C. Hendrix, H. Rosemeyer, I. Verheggen, F. Seela, A. Van Aerschot, P. Herdewijn, *Chem. Eur. J.* **1997**, *3*, 110–120.

[7] a) E. Lescrinier, R. Esnouf, J. Schraml, R. Busson, H. A. Heus, C. W. Hilbers, P. Herdewijn, *Chem. Biol.* **2000**, *7*, 719–731; b) C. Hendrix, H. Rosemeyer, B. De Bouvere, A. Van Aerschot, F. Seela, P. Herdewijn, *Chem. Eur. J.* **1997**, *3*, 1513–1520.

[8] Y. Maurinsh, H. Rosemeyer, R. Esnouf, A. Medvedovici, J. Wang, G. Ceulemans, E. Lescrinier, C. Hendrix, R. Busson, P. Sandra, F. Seela, A. Van Aerschot, P. Herdewijn, *Chem. Eur. J.* **1999**, *5*, 2139–2150.

[9] B. Allart, K. Khan, H. Rosemeyer, G. Schepers, C. Hendrix, K. Rothenbacher, F. Seela, A. Van Aerschot, P. Herdewijn, *Chem. Eur. J.* **1999**, *5*, 2424–2431.

[10] J. Wang, B. Verbeure, I. Luyten, E. Lescrinier, M. Froeyen, C. Hendrix, H. Rosemeyer, F. Seela, A. Van Aerschot, P. Herdewijn, *J. Am. Chem. Soc.* **2000**, *122*, 8595–8602.

[11] a) M. D. Sørensen, L. Kværnø, T. Bryld, A. E. Håkansson, B. Verbeure, G. Gaubert, P. Herdewijn, J. Wengel, *J. Am. Chem. Soc.* **2002**, *124*, 2164–2176; b) N. K. Christensen, T. Bryld, M. D. Sørensen, K. Arar, J. Wengel, P. Nielsen, *Chem. Commun.* **2004**, 282–283.

[12] M. Froeyen, F. Morvan, J.-J. Vasseur, P. Nielsen, A. Van Aerschot, H. Rosemeyer, P. Herdewijn, *Chem. Biodiversity* **2007**, *4*, 803–817.

[13] S. Klussmann, in *Highlights in Bioorganic Chemistry: Methods and Applications* (Eds.: C. Schmuck, H. Wennemers), Wiley-VCH, Weinheim, **2004**.

[14] Y. Kim, C. J. Yang, W. Tan, *Nucleic Acids Res.* **2007**, *35*, 7279–7287.

[15] Given the high affinity of D-HNA for natural complements, particularly D-RNA, see refs. [6,7] and: G. Kolb, S. Reigadas, C. Boiziau, A. van Aerschot, A. Arzumanov, M. J. Gait, P. Herdewijn, J.-J. Toulmé, *Biochemistry* **2005**, *44*, 2926–2933, it can be anticipated that the L-HNA system presents the proper requirements to hybridize with L-RNA with high affinity, and therefore to be conveniently used as a spiegelmer construct.

[16] For a review, see: D. D'Alonzo, A. Guaragna, G. Palumbo, *Curr. Org. Chem.* **2009**, *13*, 71–98.

[17] D. D'Alonzo, A. Guaragna, A. Van Aerschot, P. Herdewijn, G. Palumbo, *Tetrahedron Lett.* **2008**, *49*, 6068–6070.

[18] A. Guaragna, C. Napolitano, D. D'Alonzo, S. Pedatella, G. Palumbo, *Org. Lett.* **2006**, *8*, 4863–4866.

[19] D. D'Alonzo, A. Guaragna, C. Napolitano, G. Palumbo, *J. Org. Chem.* **2008**, *73*, 5636–5639.

[20] H. Takahata, Y. Banba, H. Ouchi, H. Nemoto, *Org. Lett.* **2003**, *5*, 2527–2529.

[21] For a similar result, see: B. Allart, R. Busson, J. Rozenski, A. Van Aerschot, P. Herdewijn, *Tetrahedron* **1999**, *55*, 6527–6546.

[22] I. Verheggen, A. Van Aerschot, S. Toppet, R. Snoeck, G. Janssen, P. Claes, J. Balzarini, E. De Clercq, P. Herdewijn, *J. Med. Chem.* **1993**, *36*, 2033–2040.

[23] Preparation of 2,3-*O*-isopropylidene-L-glyceraldehyde, which is the starting material of the synthesis, has been reported to lead in some cases to partial racemisation, see: C. Hubschwerlen, J.-L. Specklin, J. Higelin, *Org. Synth.* **1995**, *72*, 1–3.

[24] a) P. Wang, J. H. Hong, J. S. Cooperwood, C. K. Chu, *Antiviral Res.* **1998**, *40*, 19–44; b) C. Mathè, G. Gosselin, *Antiviral Res.* **2006**, *71*, 276–281; c) E. Sabini, S. Hazra, M. Konrad, A. Lavie, *J. Med. Chem.* **2007**, *50*, 3004–3014.

[25] Compounds **13** and **14** had already been evaluated as potential inhibitors of HIV (strain IIIB in MT4 cells), HCMV (strain AD169 in MRC5 cells) and HSV-1 (Vero cells) infections. Unfortunately, they were inactive in these assays, see: M. W. Andersen, S. M. Daluge, L. Kerremans, P. Herdewijn, *Tetrahedron Lett.* **1997**, *38*, 8147–8150. In our hands, these compounds were also found inactive against para-influenza-3, reovirus-1, Sindbis and Punta Toro viruses (Vero cells), feline corona and feline herpes viruses (CRFK cells), HSV-1, HSV-2 and vaccinia virus (Hel cells), respiratory syncytial virus (HeLa cells), vesicular stomatitis virus (Hel and HeLa cells), coxsackie B4 virus (Vero and HeLa cells), influenza A H1N1 subtype, influenza A H3N2 subtype and influenza B viruses (MDCK cells).

[26] G. S. Ti, B. L. Gaffney, R. A. Jones, *J. Am. Chem. Soc.* **1982**, *104*, 1316–1319.

[27] M. Gait, *Oligonucleotides: A Practical Approach*, IRL, Oxford, **1984**.

[28] A. Van Aerschot, T. Saison-Behmoaras, J. Rozenski, C. Hendrix, G. Schepers, G. Verhoeven, P. Herdewijn, *Bull. Soc. Chim. Belges* **1995**, *104*, 717–720.

[29] Hybridisation with unnatural oligonucleotides, which has been primarily carried out for the in-depth examination of heterochiral associations, can have several applications. As mentioned before, investigations have already been carried out to study the conformational and/or chiral selection of oligonucleotides (see ref. [12]). Depending on the opportunity to have an orthogonal oligonucleotide pairing system, such as β-D-homo-DNA, useful practical applications as molecular beacons in DNA diagnostics have also been developed: C. Crey-Desbiolles, D.-R. Ahn, C. J. Leumann, *Nucleic Acids Res.* **2005**, *33*, e77.

[30] K. Groebke, J. Hunziker, W. Fraser, L. Peng, U. Diederichsen, K. Zimmermann, A. Holzner, C. Leumann, A. Eschenmoser, *Helv. Chim. Acta* **1998**, *81*, 375–473.

[31] J. J. Vasseur is kindly acknowledged for the generous gift of L-DNA (dT_{10}).

[32] a) M. Egholm, O. Buchardt, P. E. Nielsen, R. H. Berg, *J. Am. Chem. Soc.* **1992**, *114*, 1895–1897; b) M. Egholm, O. Buchardt, L. Christensen, C. Behrens, S. M. Freier, D. A. Driver, R. H. Berg, S. K. Kim, B. Norden, P. E. Nielsen, *Nature* **1993**, *365*, 566–568.

[33] L. Kerremans, G. Schepers, J. Rozenski, R. Busson, A. Van Aerschot, P. Herdewijn, *Org. Lett.* **2001**, *3*, 4129–4132.

[34] This represents a further proof of the enantiomeric purity of the synthesised L-HNA.

[35] This result disagrees with previous experiments on the thermal behaviour of the enantiomer oligo-d($\mathbf{A}_D$*)$_{13}$ (ref. [6]), in which a d-($\mathbf{A}_D$*)$_{13}$–d($\mathbf{A}_D$*)$_{13}$ interaction was not found (even though it was not completely excluded). As two enantiomers must have the same thermal behaviour, d($\mathbf{A}_D$*)$_{13}$–d($\mathbf{A}_D$*)$_{13}$ hybridisation was again studied and found to have the same complex d($\mathbf{A}_L$*)$_{13}$–d($\mathbf{A}_L$*)$_{13}$ (Table 3).

[36] The 6′-d($\mathbf{A}_L$*($\mathbf{T}_L$*)$_3$$\mathbf{A}_L$*$\mathbf{T}_L$*$\mathbf{A}_L$*($\mathbf{T}_L$*)$_2$$\mathbf{A}_L$*($\mathbf{T}_L$*)$_2$$\mathbf{A}_L$*) strand on its own gave a T_m of 50.5 °C; considering that the latter is a noncomplementary system, an overhanged Watson–Crick base pairing (provided with some mismatches) of two separate strands can be conjectured:

[37] The weak association reported in Table 4 (entry 4) most probably

6'-ATTTATATTATTA-4'
4'-ATTATTATATTTA-6'

corresponds to ds-L-HNA-($\mathbf{A}$*)$_{13}$, which had very similar melting curves.

[38] This weak association is again probably related to ds-L-HNA-($\mathbf{A}$*)$_{13}$.

[39] This result is corroborated by the X-ray analysis of ds-D-HNA, which has demonstrated that the latter forms a right-handed double helix: R. Declercq, A. Van Aerschot, R. J. Read, P. Herdewijn, L. Van Meervelt, *J. Am. Chem. Soc.* **2002**, *124*, 928–933.

[40] The accurate amount of double strand compared to that of the single strands in each LC-MS experiment can obviously depend on how stable the complex is, and therefore this experiment should not be taken into account for a quantitative analysis.

Received: July 3, 2009
Published online: September 8, 2009

